Journal of Coordination Chemistry

ISSN: 0095-8972 (Print) 1029-0389 (Online) Journal homepage: http://www.tandfonline.com/loi/gcoo20

Elaborated spectral analysis and modeling calculations on Co(II), Ni(II), Cu(II), Pd(II), Pt(II), and Pt(IV) nanoparticles complexes with simple thiourea derivative

Gamil A.A. Al-Hazmi, Adel A. El-Zahhar, Khlood S. Abou-Melha, Fawaz A. Saad, Mohamed H. Abdel-Rhman, Abdalla M. Khedr & Nashwa M. El-Metwaly

To cite this article: Gamil A.A. Al-Hazmi, Adel A. El-Zahhar, Khlood S. Abou-Melha, Fawaz A. Saad, Mohamed H. Abdel-Rhman, Abdalla M. Khedr & Nashwa M. El-Metwaly (2015) Elaborated spectral analysis and modeling calculations on Co(II), Ni(II), Cu(II), Pd(II), Pt(II), and Pt(IV) nanoparticles complexes with simple thiourea derivative, Journal of Coordination Chemistry, 68:6, 993-1009, DOI: 10.1080/00958972.2015.1004325

To link to this article: http://dx.doi.org/10.1080/00958972.2015.1004325

View supplementary material

Accepted author version posted online: 09 Jan 2015.
Published online: 02 Feb 2015.

Submit your article to this journal

Article views: 61

View related articles

View Crossmark data

Full Terms & Conditions of access and use can be found at
http://www.tandfonline.com/action/journalInformation?journalCode=gcoo20

Download by: [Mizoram University]

Date: 28 December 2015, At: 14:52

Journal of Coordination Chemistry, 2015
Vol. 68, No. 6, 993–1009, http://dx.doi.org/10.1080/00958972.2015.1004325

Taylor & Francis
Taylor & Francis Group

Elaborated spectral analysis and modeling calculations on Co(II), Ni(II), Cu(II), Pd(II), Pt(II), and Pt(IV) nanoparticles complexes with simple thiourea derivative

GAMIL A.A. AL-HAZMI†‡, ADEL A. EL-ZAHHAR‡§, KHLOOD S. ABOU-MELHA‡, FAWAZ A. SAAD¶, MOHAMED H. ABDEL-RHMAN‖, ABDALLA M. KHEDR¶†† and NASHWA M. EL-METWALY*¶‖

†Faculty of Applied Sciences, Chemistry Department, Taiz University, Taiz, Yemen
‡Faculty of Science, Chemistry Department, King Khalid University, Abha, Saudi Arabia
§Nuclear Chemistry Department, Hot Lab. Center, EAEA, Cairo, Egypt
¶Chemistry Department, College of Applied Sciences, Umm Al-Qura University, Makkah, Saudi Arabia
‖Faculty of Science, Chemistry Department, Mansoura University, Mansoura, Egypt
††Faculty of Science, Chemistry Department, Tanta University, Tanta, Egypt

(*Received 17 September 2014; accepted 12 December 2014*)

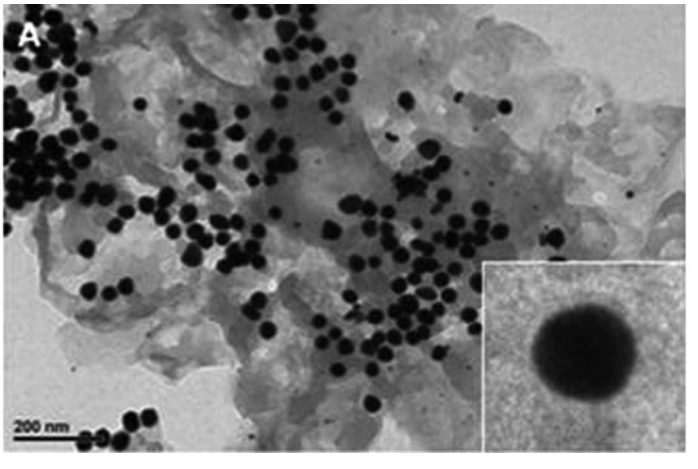

Transmission electron micrographs of the Pt(IV) complex; inset shows the magnified image.

A series of metal complexes was synthesized using a simple thiourea derivative. The prepared complexes were characterized using different techniques (FTIR, ESR, X-ray diffraction [XRD], TG/DTA, and TEM). The FTIR spectrum of the ligand shows the presence of its tautomer forms (keto–enol). The ligand coordinates as a neutral bidentate in the Pt(IV), Pd(II), and Pt(II) complexes. In the case of Co(II) and Ni(II) complexes, the ligand is mono-negative bidentate. The proposed complexes are four to six coordinate. The geometries are proposed based on electronic spectral data and magnetic measurements and were verified using other tools. The XRD patterns reflect the

*Corresponding author. Email: n_elmetwaly00@yahoo.com

© 2015 Taylor & Francis

Downloaded by [Mizoram University] at 14:52 28 December 2015

nanocrystalline structures except for the Cu(II) complex, which is amorphous. The TEM images for platinum complexes show nanosize particles and homogeneous metal ion distribution on the complex surface. The EPR spectrum of Cu(II) complex verified the octahedral geometry of the complex. Molecular modeling was performed to assign the structural formula proposed for the ligand based on the characterization results.

Keywords: Thiourea complexes; X-ray diffractions; Molecular modeling

Downloaded by [Mizoram University] at 14:52 28 December 2015

1. Introduction

Complexes of organic compounds containing oxygen, nitrogen, and sulfur donors [1] show effects of sulfur and electron delocalization in potential biological activity. Thiourea is recognized for inter- and intra-molecular hydrogen-bonding and as ligands in coordination complexes, leading to their use in self-assembled network materials [2]. Thiourea complexes with transition metal atoms are also of interest because of the special roles played by these compounds in biological processes [3–5]. Thiourea derivatives have many polar intermolecular binding sites to develop molecular (self) recognition. As a consequence, thiourea metal complexes present attractive features related to the specific binding modes and to biological properties [6]. Many thiourea complexes of Pt^{+2} and Pd^{+2} have H-bonding and other inter-molecular interactions; many of these complexes change their solid state structure in the presence of different counterions and/or solvents [7–10]. Potential N-metal coordination [11, 12] enables some thiourea complexes to cluster via thiourea bridges, yielding an important class of metal cages able to selectively recognize (and also detect) specific anions [13, 14]. Complexes containing d^8 metal–sulfur bonds bear potential anti-cancer activity [15, 16] as S-donor ligands are strong competitors for metal coordination sites [17, 18]; indeed, in physiological media, thiourea complexes could be drug reservoirs and/or reduce metal toxicity [19–21]. Our goal was to synthesize a series of thiourea complexes. The complexes are investigated using spectral techniques. X-ray diffraction (XRD) and TEM analysis give insight about the crystal nature. Molecular modeling calculations are performed to verify the proposed structures.

2. Theoretical

2.1. *Molecular modeling*

Geometry optimization and conformational analysis have been performed by the use of semi-empirical PM3 [22] force field as implemented in Hyper-Chem 7.5 [23], also, the molecular parameters are calculated.

3. Experimental

3.1. *Spectral measurements*

3.1.1. Elemental analysis. Carbon, hydrogen, and nitrogen were analyzed using a Perkin-Elmer CHN 2400 in the Micro-analytical Unit at the Faculty of Science, Cairo University,

Egypt. The metal content was determined using complexometric titrations, and the Cl content was tested gravimetrically using $AgNO_3$ [24].

3.1.2. Molar conductance. The molar conductivities of freshly prepared 1.0×10^{-3} M L^{-1} DMSO solutions were measured using a Jenway 4010 conductivity meter.

3.1.3. IR spectra. The infrared spectra, as KBr disks, were recorded on a Mattson 5000 FTIR spectrometer (400–4000 cm^{-1}), Mansoura University.

3.1.4. ^{1}H NMR and ^{13}C NMR. The proton NMR spectra were recorded on a Varian FT-500 MHz spectrometer in d_6-DMSO as a solvent and TMS as internal standard, King Khalid University.

3.1.5. Electronic spectra. The electronic spectra were recorded in DMSO from 200 to−900 nm using a Unicam UV–vis spectrometer, Mansoura University.

3.1.6. Magnetic measurements. The effective magnetic moments (BM) were evaluated at room temperature by applying $\mu_{\text{eff}} = 2.8\sqrt{X_{\text{M}}T}$, where X_{M} is the molar susceptibility corrected using Pascal's constants for the diamagnetism of all atoms in the ligand using a Johnson Matthey magnetic susceptibility balance.

3.1.7. Thermal analysis. Differential thermal analysis (DTA) and thermogravimetric analysis (TGA) experiments were conducted using Shimadzu DTA-50 and Shimadzu TGA-50H thermal analyzers, respectively, at Micro Analytical Center, King Khalid University. All experiments were performed using a single loose top loading platinum sample pan under nitrogen at a flow rate of 30 mL min^{-1} and a 10 °C min^{-1} heating rate for the temperature range 25–800 °C.

3.1.8. ESR spectrum. ESR spectrum of solid Cu(II) complex was obtained on a Bruker EMX spectrometer working in the X-band (9.78 GHz) with 100 kHz modulation frequency. The microwave power was set at 1 mW, and modulation amplitude was set at 4 gauss. The low field-signal was obtained after 4 scans with a 10-fold increase in the receiver gain. A spectrum was obtained in a 2-mm quartz capillary at room temperature, Tanta University.

3.1.9. X-ray diffractions. XRD patterns of the samples were recorded on a X'Pert Philips X-ray diffractometer. All patterns were obtained using Cu/Kα1 radiation with a graphite monochromator at 0.02° min^{-1} scanning rate. The metal complexes were made in the form of tablets, which have ≈0.1 cm thickness, under a pressure of approximately 5×10^7 Pa, King Khalid University.

Downloaded by [Mizoram University] at 14:52 28 December 2015

3.1.10. Transmittance electron microscopy (TEM). Transmittance electron microscopy (TEM) images were taken with Jeol JSM-6390 equipment.

3.2. *Reagents*

Benzoyl chloride, NH_4SCN, and *p*-chloroaniline were of analytically reagent grade, commercially available from Fulka, and used without purification. $Co(NO_3)_2{\cdot}6H_2O$, $Ni(OAc)_2{\cdot}4H_2O$, $Cu(OAc)_2{\cdot}H_2O$, $PtCl_2$, $PdCl_2$, and $PtCl_4$ salts were purchased from Merck Co.

3.3. *Synthesis of H_2BCT ligand*

In a round bottom flask, 4.086 g of NH_4SCN (0.055 M) was added to 80 mL of dry acetone. Benzoylchloride (0.05 M) was added dropwise under stirring and heating for 15 min. *p*-chloroaniline (0.05 M) was added and heated again for further 30 min; afterward, it was allowed to cool and all contents were poured onto ice water. The product was collected by filtration, washed with bidistilled water and ether, and recrystallized in ethanol. The isolated 1-benzoyl-3-(4-chlorophenyl)thiourea ($C_{14}H_{11}N_2SOCl$) [figure 1(A) and (B)] by 68% yield has a m.p. = 154–155 °C and elemental analysis of: C 57.83, H 3.82, N 9.63. The ^{1}H NMR spectrum (d_6-DMSO, 500 MHz) given in figure 2(A) showed (δ, ppm) 12.7 (s, 1H, OH), 11.7 (s, 1H, NH^1), 7.99 (s, 1H, NH^3), 7.73–7.89 (m, 4H, Ph-Cl), 7.69–7.48 (m, 5H, Ph), 3.4(DMSO), and 2.6 (H_2O in DMSO). The absence of any peak assigned to SH proton (δ = 1–1.5 ppm) supports lack of thione–thiol tautomer forms. ^{13}C NMR (ppm) showed

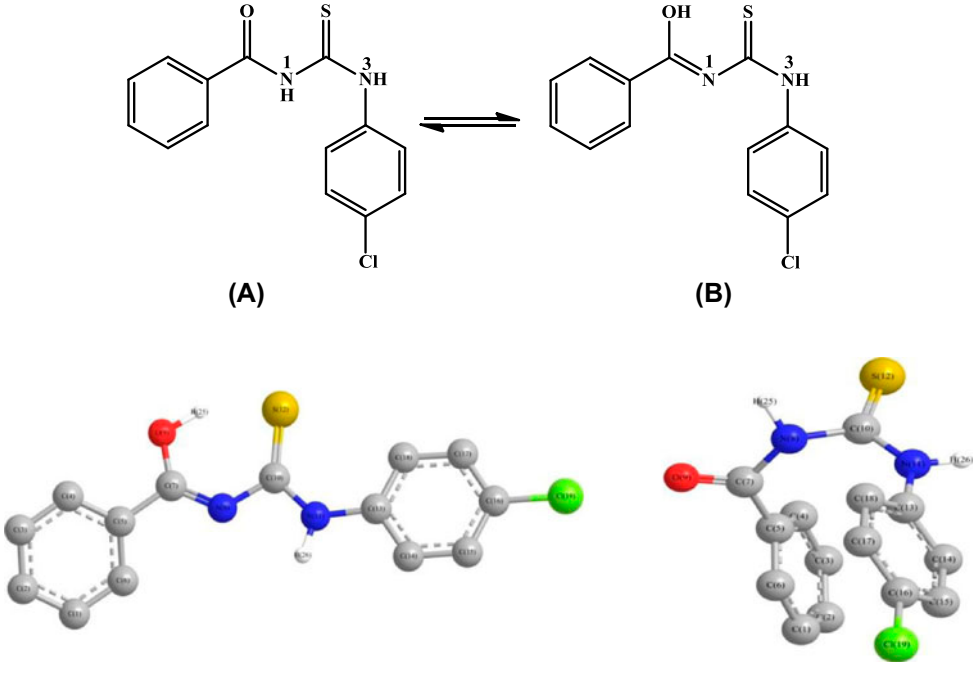

Figure 1. The structural form of 1-benzoyl-3-(4-chlorophenyl)thiourea, H_2BCT and its molecular keto (A)–enol (B) modeling.

Downloaded by [Mizoram University] at 14:52 28 December 2015

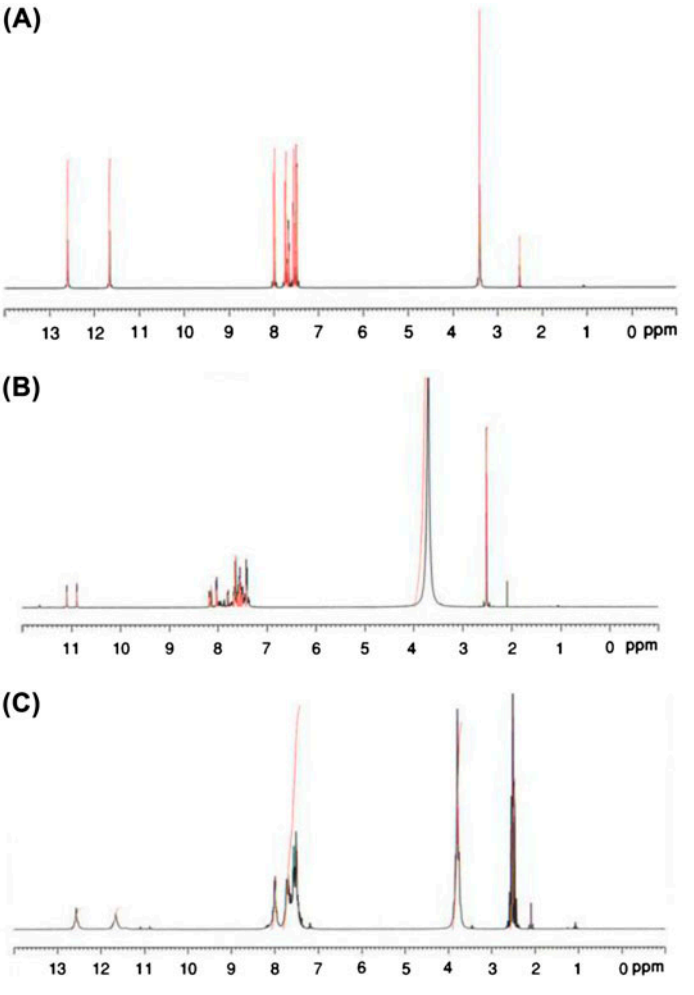

Figure 2. The ^{1}H NMR spectra of the (A) free ligand, (B) Pt(IV) and (C) Pd(II) complexes.

peaks at 179.3 (C=S), 168.2 (C=O), 136.9 (C–OH), 126.2–133.1(Ph carbons), and 38.98–39.98 (DMSO).

Calculated distribution of activity scores (version 2011.06) for GPCR ligands, kinase inhibitors, ion channel modulators, nuclear receptor ligands, protease inhibitors, and other enzyme targets was compared with scores for about 100,000 average drug-like molecules. The score allows efficient separation of active and inactive molecules. The results show the following: GPCR (G protein-coupled receptor) ligand −0.38, ion channel modulator −0.34, kinase inhibitor −0.28, nuclear receptor ligand −0.70, protease inhibitor −0.57, and enzyme inhibitor −0.27.

3.4. *Synthesis of metal complexes*

The M- H_2BCT complexes were prepared by refluxing H_2BCT (0.582 g, 2 mM) with 2 mM of each metal salt; 0.216 g of $Co(NO_3)_2{\cdot}6H_2O$, 0.498 g of $Ni(OAc)_2{\cdot}4H_2O$, 0.399 g

Downloaded by [Mizoram University] at 14:52 28 December 2015

of $Cu(OAc)_2 \cdot H_2O$, 0.355 g of $PdCl_2$, 0.532 g of $PtCl_2$, and 0.674 g of $PtCl_4$ in 20 mL ethanol for 3 h. A little solid KCl was added with Pt(II), Pt(IV), and Pd(II) salts for complete dissolution. The resulting metal complexes were filtered off while hot, washed with ethanol followed by diethyl ether, and dried in vacuum over $CaCl_2$. ^{1}H NMR spectrum of Pt(IV) complex (d_6-DMSO, 500 MHz) given in figure 2(B) shows (δ, ppm) the following: 11.2 (s, 2H, $2NH^3$), 10.9 (s, 2H, 2OH), 8.02–8.19 (m, 8H, 2Ph-Cl), 7.41–7.81 (m, 10H, 2Ph), 2.51 (DMSO), and 3.7 (H_2O). The ^{13}C NMR showed bands at (δ, ppm): 168 (C=S), 151 (C=O), 136.7 (C–OH), 121.4–127.4 (2Ph), 128.2–133.1 (2Ph-Cl), and 38.98–40.07 (DMSO). The ^{1}H NMR of Pd(II) complex (d_6-DMSO, 500 MHz) given in figure 2(C) shows the peaks at (δ, ppm): 12.6 (s, 2H, 2OH), 11.7 (s, 2H, $2NH^3$), 7.67–8.00 (m, 8H, 2Ph-Cl), 7.49–7.58 (m, 10H, 2Ph), 3.8 (DMSO), 2.65 (H_2O). The ^{13}C NMR shows the peaks (δ, ppm): 160 (C=S), 152 (C=O), 126.5 (C–OH), 128.6 (Ph groups), and 40.01 (DMSO).

4. Results and discussion

The physical properties of the prepared thiourea complexes were investigated and summarized in table 1. The elemental analysis showed that the formed complexes are by 1 : 2 (M : L) molar ratio.

4.1. *Molar conductance*

Conductivity measurements were performed for clear solution in DMSO as a solvent at room temperature. The molar conductivity values for 10^{-3} M L^{-1} of Pd(II) and Pt(IV) complexes were 115.3 and 118 Ohm^{-1} cm^2 M^{-1}, respectively, suggesting the electrolytic nature of these complexes [25], while the other complexes show values indicating their non-electrolytic nature [26]. The use of chloride salts favors conductance of the complexes.

4.2. *IR, ^{1}H NMR, and ^{13}C NMR spectra*

Infrared absorption spectra are an important tool to determine the mode of chelation. The H_2BCT spectrum displays significant bands supporting the presence of two tautomeric forms (keto and enol) [27]. The absence of a band around 2400 cm^{-1} (υSH) also supports the keto–enol form as the only tautomer proposed. Bands at 1676, 1531, 1092, and 784 cm^{-1} are assigned for υC=O, υC=N, υC–O, and υC = S, respectively. Broadness around 1750 cm^{-1} suggests intra-ligand H-bonding. These data are consistent with ^{1}H NMR and ^{13}C NMR results discussed in the Experimental section. The elemental analysis shows two ligands coordinating with each central atom. The significant bands abstracted from a comparative spectral study are summarized in table 2. All metal complexes spectra display a broad band at 3440–3100 cm^{-1}, which could be attributed to υOH of water [28], suggesting the presence of lattice and/or coordinated water in these complexes. Crystal water appears at frequencies higher than that of the coordination water. The major vibration modes at 3420–3370 cm^{-1} are evidence of the presence of lattice water in all complexes except Ni(II). These non-ligand bands can be interpreted in terms of the presence of lattice and coordinated water, also supported through the thermal decomposition. For Pd(II), Pt(II), and

Downloaded by [Mizoram University] at 14:52 28 December 2015

Downloaded by [Mizoram University] at 14:52 28 December 2015

Table 1. Analytical data for H_2BCT and its complexes.

No.	Compound	Color	Elemental analysis (%) Calcd (Found)					Λ_M (Ω^{-1} cm^2 M^{-1})
			C	H	N	M	Cl	
1	H_2BCT	Creamy	57.83 (57.82)	3.81 (3.80)	9.63 (9.63)	–	–	2.3
2	$[Co(HBCT)_2]\cdot 2H_2O$	Dark green	49.86 (49.85)	3.59 (3.58)	8.31 (8.30)	8.74 (8.75)	–	5.2
3	$[Ni(HBCT)_2(H_2O)_2]$	Faint green	49.88 (49.86)	3.59 (3.58)	8.31 (8.30)	8.70 (8.70)	–	–
4	$[Cu(H_2BCT)_2(OAc)_2]\cdot 2H_2O$	Green	48.09 (48.10)	4.03 (4.05)	7.01 (7.02)	7.95 (7.93)	–	–
5	$[Pd(H_2BCT)_2]Cl_2\cdot 2H_2O$	Yellow	36.26 (36.25)	3.29 (3.29)	7.05 (7.05)	13.39 (13.38)	8.92 (8.91)	115.3
6	$[Pt(H_2BCT)_2Cl_2]\cdot 2H_2O$	Faint green	38.06 (38.04)	2.96 (2.96)	6.34 (6.33)	22.08 (22.09)	8.03 (8.02)	–
7	$[Pt(H_2BCT)_2Cl_2]Cl_2\cdot 2H_2O$	Yellow	35.23 (35.22)	2.74 (2.72)	5.87 (5.86)	20.44 (20.43)	7.43 (7.44)	118

Downloaded by [Mizoram University] at 14:52 28 December 2015

Table 2. Assignments of the IR significant bands (cm^{-1}) of H_2BCT and its metal complexes.

Assignments	H_2BCT	Co(II)	Ni(II)	Cu(II)	Pd(II)	Pt(II)	Pt(IV)
ν^1(NH), ν^3(NH) + ν_{as}(OH); H_2O or C–OH	3407 3264	3400	3380	3370	3420	3400	3380
δ(O H); H_2O	–	1384	1376	1350	1349	1350	1332
ν(C=O)(amide)	1676	–	–	1630	–	1660	1668
ν(C=S) (I; II; IV)	1531	1510	1489	1523	1533	1520	1489
	1260	1210	1235	1236	1256	1253	1260
	784	750	770	756	754	760	752
ν(C=N)	–	1560	1590	–	1560	1560	1580
ν(C–O)	–	1033	1013	–	1190	1120	1130
$\delta_r(H_2O)$ and $\delta_w(H_2O)$	–	676	682	660	662	690	659
Ring deformation	–	935	916	950	946	930	956
ν(M–O) + ν(M–S)	–	485,420	485,455	500,480	510,481	500,460	540,480

Downloaded by [Mizoram University] at 14:52 28 December 2015

Pt(IV) complexes, bands assigned for υC=N, υC–O, and δOH with shifted band for υC=O [29, 30] suggest coordination of ligands by two tautomer forms (keto–enol). This behavior is due to the presence of relatively acidic medium produced by chloride salts. The Cu(II) complex spectrum has the shift of υC=O to lower wavelengths as well as no υC=N and υC–O bands, indicating coordination of the ligand in its keto form only. Bands at 1450 and 1700 cm^{-1} assigned to υ_{sym} and υ_{asym}(OAc), respectively, reflect the contribution of monodentate acetate [31]. The shift of υC=S(I–IV) bands, especially the forth one, to lower wavelengths suggests coordination. In spectra of Ni(II) and Co(II) complexes, no υC=O band was observed, suggesting its ionization during coordination. Also, bands attributed to υC=N and υC–O are further support. Finally, new bands at lower frequency assigned to υM–O and υM–S vibrations were observed. In the Pt(IV) and Pd(II) complexes, the mode of bonding is verified by ^{1}H NMR and ^{13}C NMR data. The shifts observed for OH (δ = 10.9 and 12.6 ppm) and NH^{3} (δ = 11.2 and 11.7 ppm), respectively, support coordinating OH with loss of inter-ligand H-bonding. Also, the ^{13}C NMR spectra display the upfield shifts for C=O, C=S, and C–OH signals.

4.3. *Electronic spectra and MB*

The electronic spectral analysis was performed in DMSO to assign the structures of the metal complexes. The results (table 3) showed that d–d splitting is strongly affected by the geometry around the metal. The spectrum of $[Co(HBCT)_2]\cdot 2H_2O$ reflects the tetrahedral geometry around Co(II) (figure 3). Bands at 15,980 and 19,150 cm^{-1} could be assigned for $^{4}A_2 \rightarrow {}^{4}T_1$ and LMCT transitions in a tetrahedral configuration [32]. The MB value (4.80 BM) gives extra evidence for this proposal. The ligand-field parameters (10Dq = 8522.5 cm^{-1}, B = 852.25 cm^{-1}, and β = 0.878) introduce the ionic character of the M–L bonds. The spectra of $[Ni(HBCT)_2(H_2O)_2]$ and $[Pt(H_2BCT)_2Cl_2]\cdot 2H_2O$ are consistent with octahedral geometry. Bands at 14,780; 15,280 and 24,800; 25,100 cm^{-1} for $^{3}A_{2\,g} \rightarrow {}^{3}T_{1\,g}$(F) and $^{3}A_{2\,g} \rightarrow {}^{3}T_{1\,g}$(P) transitions, respectively [33], are consistent with octahedral configurations. The ligand-field parameters (10Dq = 9069.1 cm^{-1}, B = 824.47 cm^{-1}, and β = 0.792) were determined. These values are in agreement with those reported for six coordination d^{8} systems with SO donors [34]. The MB values (2.90 and 3.10 BM) confirm further the suggestion (figure 3).

The spectrum of $[Cu(H_2BCT)_2(OAc)_2]\cdot 2H_2O$ reflects a distorted octahedral geometry (μ_{eff} = 1.81 BM). This is based on the appearance of broad bands centered at 15,385 and 24,778 cm^{-1} and attributed to $^{2}E_{2\,g} \rightarrow {}^{2}T_{2\,g}$ and LMCT transitions, respectively [35–37]. Previous studies on Cu(II) complexes [38] [figure 4(A)] reported that the band at

Table 3. BM and electronic spectral bands (cm^{-1}) of the ligand and its complexes.

Compound	μ_{eff} (BM)	d–d transition (cm^{-1})	Intra-ligand and charge transfer (cm^{-1})
1	–	–	33,333; 26,316
2	4.8	19,150; 15,980	33,000; 27,310
3	2.9	14,780; 24,800	32,560; 27,410
4	1.8	14,385	32,303; 26,256; 24,778
5	0.0	–	32,500; 25,000; 20,000
6	3.1	15,280; 25,100	33,300; 27,100
7	0.0	–	25,250; 24,040

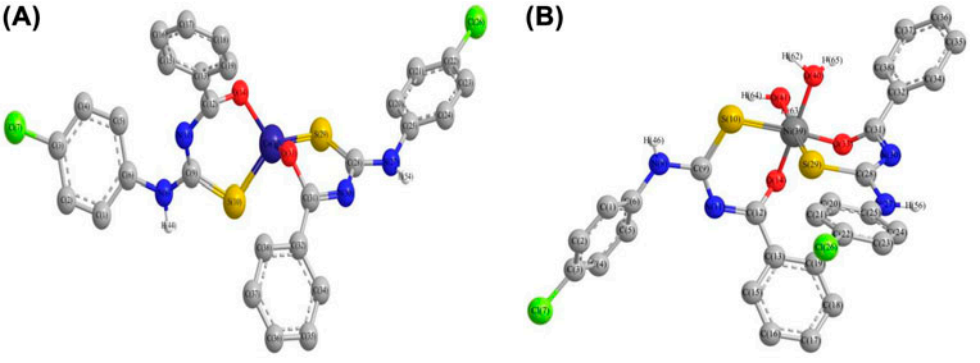

Figure 3. The proposed structural formula of Co(II) (A) and Ni(II) (B) complexes.

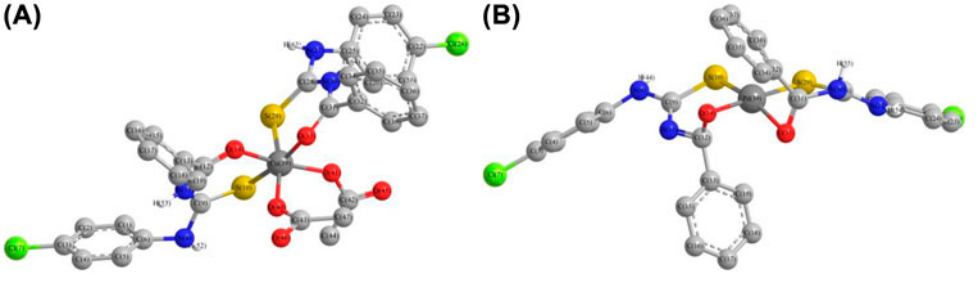

Figure 4. The proposed structures of Cu(II) (A) and Pd(II) (B) complexes.

21,785–24,750 cm^{-1} was attributed to S → Cu(II) transition similar to the value of our complex. The electronic spectrum of $[Pd(H_2BCT)_2]Cl_2{\cdot}2H_2O$ is indicative of a square–planar geometry. Strong charge-transfer transition interferes with observation of the expected bands. A very intense band at 20,000 cm^{-1} could be assigned to S → M(II) and O → M(II) charge-transfer and d–d bands. A strong band at 25,000 cm^{-1} could be assigned to the combination of metal–ligand charge-transfer bands. A band at

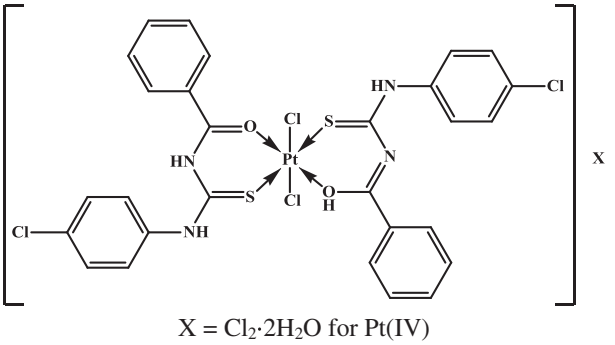

X = $Cl_2{\cdot}2H_2O$ for Pt(IV)

X = $2H_2O$ for Pt(II)

Figure 5. The proposed structural formula of Pt(IV) and Pt(II) complexes.

Downloaded by [Mizoram University] at 14:52 28 December 2015

32,500 cm^{-1} is assigned to $n \rightarrow \pi^*$ transition of the phenyl rings with thiourea moiety (L → MCT). The spectrum of the ligand shows $\pi \rightarrow \pi^*$ and $n \rightarrow \pi^*$ transition bands at 33,333 and 26,316 cm^{-1} [figure 4(B)].

The spectrum of $[Pt(H_2BCT)_2Cl_2]Cl_2 \cdot 2H_2O$ shows a band at 25,250 cm^{-1} assigned to $n \rightarrow \pi^*$ transition, while the band at 24,040 cm^{-1} may be attributed to LMCT. Previous studies on Pt(IV) complexes reported that the band at 25,000–26,040 cm^{-1} was assigned for S(σ) → M transition and the band at 20,600 cm^{-1} was due to S(π) → M transition [39, 40]. Moreover, the band at 21,790–24,750 cm^{-1} was assigned to O → M(II) transition in an octahedral geometry (figure 5).

4.4. *Thermal behavior*

The TG and DTG analysis were performed for the ligand and its metal complexes to describe the thermal stability of all prepared compounds. The TG curve of the ligand shows a complete decomposition in one step, while the complexes were stepwisely degraded. The plausible decomposition behavior was interpreted to the data represented in table 4. The data reveal the lower thermal stability except for Ni(II) complex. The degradation process

Table 4. TGA data of all investigated compounds.

Compound	Steps	Temp. range (°C)	Decomposed assignments	Weight loss found (Calcd %)
1	1st	150–330	$-C_{14}H_{11}N_2SOCl$	100 (100)
2	1st	75–310	$-2H_2O + C_{12}H_9Cl$	33.30 (33.31)
	2nd	360–395	$-C_{12}H_9Cl$	27.96 (27.97)
	3rd	398–727	$-C_2HN_2OS$	14.99 (14.99)
	Residue	At 730	$Co(C_2HN_2OS)$	23.75 (23.73)
3	1st	130–320	$-2H_2O + C_{12}H_9Cl$	33.65 (33.32)
	2nd	330–462	$-C_{12}H_9Cl$	27.10 (27.98)
	3rd	460–680	$-C_4H_2N_4OS_2$	26.97 (27.62)
	Residue	At 770	NiO	12.28 (11.08)
4	1st	75–335	$-2H_2O + 2(OAc) + C_{12}H_9Cl$	43.23 (42.89)
	2nd	426–449		23.51 (23.60)
	3rd	449–495	$-C_{12}H_9Cl$	12.72 (12.78)
	4th	581–621	$-C_2H_2N_2OS$	10.67 (10.77)
	Residue	At 800	CuO	9.87 (9.95)
5	1st	35–83	$-2H_2O$	5.09 (4.53)
	2nd	246–291	$-Cl_2 + C_{12}H_9Cl$	32.64 (32.65)
	3rd	349–380	$-C_2H_2N_2S + C_{12}H_9Cl$	34.52 (34.56)
	4th	407–559	$-C_2H_2N_2SO$	12.63 (12.85)
	Residue	At 800	PtO	15.12 (15.40)
6	1st	29–122	$-2H_2O$	4.25 (4.08)
	2nd	120–320	$-Cl_2 + C_{12}H_9Cl$	29.01 (29.37)
	3rd	350–435	$-C_2H_2N_2S + C_{12}H_9Cl$	31.11 (31.09)
	4th	430–620	$-C_2H_2N_2SO$	11.14 (11.56)
	Residue	At 800	PtO	24.49 (23.89)
7	1st	80–230	$-2H_2O + Cl_2$	11.10 (11.20)
	2nd	279–320	$-Cl_2 + C_{12}H_9Cl$	27.10 (27.19)
	3rd	459–556	$-C_2H_2N_2S + C_{12}H_9Cl$	28.77 (28.78)
	4th	670–692	$-C_2H_2N_2SO$	11.01 (10.69)
	Residue	At 750	PtO	22.02 (22.12)

Downloaded by [Mizoram University] at 14:52 28 December 2015

was started at lower temperature (~100 °C) which could be attributed to the presence of crystal water. The metal oxide is proposed as the residue of decomposition process.

4.5. *Effect of ionic radii*

The thermal stability of the metal complexes may be attributed to the ionic radii of the central metal ions. It was observed that the greater the ionic radius of the metal ion, the lower the thermal stability, with the following thermal stability orders: Pt(II) < Pd(II) < Co(II) = Cu(II) < Pt(IV) < Ni(II).

4.6. *ESR spectrum of $[Cu(H_2BCT)_2(OAc)_2]\cdot 2H_2O$*

The spin Hamiltonian parameters for $[Cu(H_2BCT)_2(OAc)_2]\cdot 2H_2O$ ($S = 1/2$, $I = 3/2$) were calculated from the powder ESR spectrum (figure 6). The g tensor values can be used to derive the ground state. In square–planar or square–pyramidal complexes, the unpaired electron lies in the $d_{x^2-y^2}$ orbital giving $^2B_{1\,g}$ as the ground state with $g_{\|} > g_{\perp} > 2.0023$, while giving $^2A_{1\,g}$ with $g_{\perp} > g_{\|} > 2.0023$ if the unpaired electron lies in the d_{z^2} orbital. The observed values, $g_{\|}$ (2.103) > $g_{\perp}$ (2.021) > 2.0023, indicate that the copper site has a $d_{x^2-y^2}$ ground state characteristic in a square–pyramidal or octahedral geometry [41]. In axial symmetry, the g values are related by: $G = (g_{\|} - 2)/(g_{\perp} - 2) = 4$, if $G > 4$, the exchange interaction between copper(II) centers in the solid state is negligible, whereas when $G < 4$, a considerable exchange interaction is indicated. The G value of the complex (5.385) suggests the absence of exchange coupling between Cu(II) centers in the solid state [42]. The tendency of $A_{\|}$(=168 × 10^{-4} cm^{-1}) to decrease with increasing $g_{\|}$ indicates increase of the tetrahedral distortion in the coordination sphere of Cu [43]. In order to quantify the degree of distortion of the Cu(II) complexes, the f factor, $g_{\|}/A_{\|}$ (an empirical index of tetrahedral distortion) [44], was selected from the ESR spectrum. Although its value ranges between 105 and 135 cm^{-1} for square–planar complexes, the values can be much larger in the presence

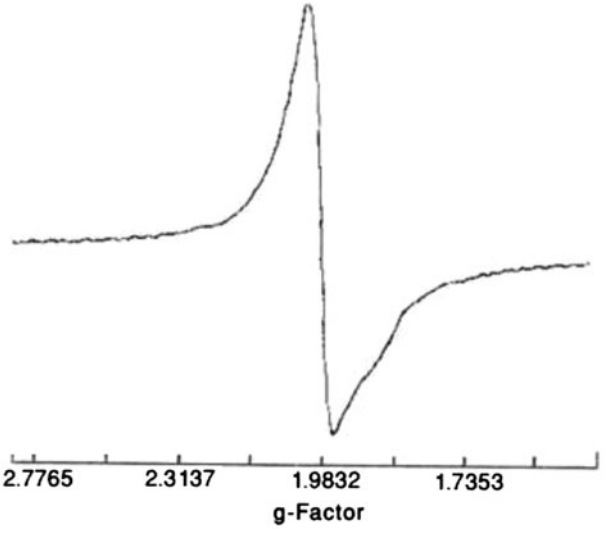

Figure 6. ESR spectrum of solid Cu(II) complex.

Downloaded by [Mizoram University] at 14:52 28 December 2015

of a tetrahedral distorted structure. For the investigated complex, the $g_{\|}/A_{\|}$ quotient is 125.18 cm^{-1} supporting the presence of significant dihedral angle distortion in the xy-plane and indicating a tetrahedral distortion from square–planar geometry. Molecular orbital coefficients, σ^2 (covalence of the in-plane σ-bonding) and β^2 (covalence of the in-plane π-bonding), were calculated using the following equations:

$$\alpha^2 = ((A_{\|}/0.036) + (g_{\|} - 2.0023) + 3/7(g_{\perp} - 2.0023) + 0.04)$$

$$\beta^2 = (g_{\|} - 2.0023)E/(-8\lambda\alpha^2).$$

The β^2 (0.206) is lower than σ^2 value (0.615), indicating more covalent character of π-bonding. The data agree with other reported values [45]. The orbital reduction factors viz., $K_{\|}$ and $K_{\perp}$, are also calculated using the following equations:

$$^2K_{\|} = (g_{\|} - 2.00277)\ E/8\lambda$$

$$^2K_{\perp} = (g_{\perp} - 2.00277)\ E/2\lambda$$

where $^2K_{\|} = \alpha^2\beta^2$ and E = 15,385 cm^{-1} (d–d transition band). For pure σ-bonding, $K_{\|} \approx K_{\perp} \approx 0.77$, while $^2K_{\|}$ (0.233) < $^2K_{\perp}$ (0.169) signifies in-plane π-bonding, with $^2K_{\perp} < {}^2K_{\|}$ accounting for out-of-plane π-bonding [46]. Furthermore, it has been reported that $g_{\|}$ is 2.4 for copper–oxygen bonds and 2.3 for copper–nitrogen bonds. In the studied complex, the $g_{\|}$ is 2.103 which may be intermediate between the O–M and S–M bonds. Finally, the g values agree with distorted octahedral geometry [47].

4.7. *XRD studies*

XRD (powder technique) can introduce important structural information about microcrystalline samples of the material under investigation [48]. The diffraction patterns were performed from $10° < 2\theta < 90°$ for the ligand and metal–ligand complexes. Comparing the XRD patterns of each ligand with its corresponding metal complexes indicates that the inter-planar spacing d (Å) and the relative intensities (I/I^0) are different from complex formation. The XRD patterns indicate crystalline nature for the investigated complexes except Cu(II), which is amorphous [49, 50]. Probably, this behavior is due to the incorporation of the water molecules. A comparative study in the patterns reflects the absence of contamination with starting materials, confirmed by known methods [51]. A shift in diffraction peaks of complexes was observed (Supplemental data), suggesting a contribution of the ligand groups. The θ, d values (the volume average of the crystal dimension normal to diffracting plane), full width at half maximum (FWHM) of prominent intensity peak, relative intensity (%), and particle size of compounds are presented in table 5. The diffraction peaks of the ligand, Pd(II), Co(II), Ni(II), Cu(II), Pt(II) and Pt(IV) ligand complexes were observed at 2θ/d-value (Å) = 18.40/4.818, 18.64/4.756, 7.40/11.937, 5.02/17.589, 20.84/4.259, 12.58/7.031, and 28.38/3.142, respectively. The crystallite size was calculated from XRD patterns by applying FWHM of the characteristic peaks using Deby–Scherrer equation: $B = 0.94\ \lambda/(S \cos\theta)$, where S is the crystallite size, θ is the diffraction angle, B is the line width at half maximum height, Cu/Kα (λ) = 1.5406 Å and the d-spacing were determined using the Bragg equation: $n\lambda = 2d\sin(\theta)$ at $n = 1$.

Downloaded by [Mizoram University] at 14:52 28 December 2015

Table 5. XRD spectral data of the highest value of intensity of the H_2BCT ligand and its complexes.

Compound	Size of particles (nm)	θ	Intensity	d-spacing (Å)	FWHM
H_2BCT	5.578	9.20	2180	4.818	0.263
Pd^{+2}–H_2L	25.438	9.32	346	4.756	0.5769
Co^{+2}–HL	60.949	3.70	500	11.937	0.2381
Ni^{+2}–HL	26.118	2.51	460	17.589	0.5550
Cu^{+2}–H_2L	15.460	10.42	316	4.259	0.9524
Pt^{+2}–H_2L	58.277	6.29	1288	7.031	0.2500
Pt^{+4}–H_2L	32.866	14.19	1436	3.142	0.4545

4.8. *Transmittance electron microscopy*

TEM is used to obtain direct information about the microstructure, surface morphology, and surface distribution of metal ions, surface homogeneity, particle size and chemical composition of compounds. The TEM images of Pt(IV) and Pt(II) complexes are presented in figure 7. These two complexes were chosen for TEM investigation after XRD indicated crystalline nature. The images show uniform and homogeneous surface and defined metal distribution on the surface of the complex. Also, it refers to the uniformity

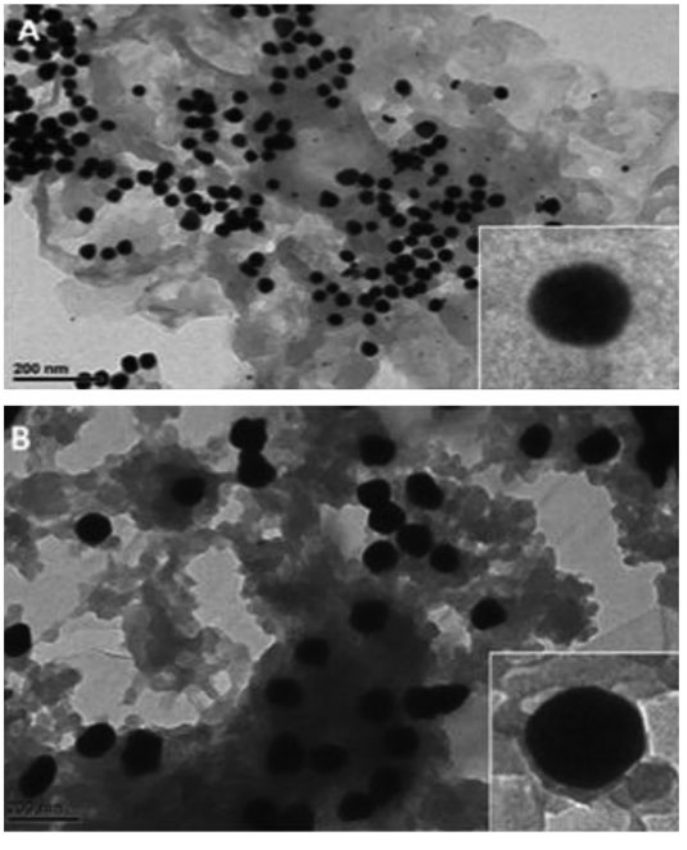

Figure 7. Transmission electron micrographs of (A) Pt(IV) and (B) Pt(II). Scale bar 200 nm. The inset shows the magnified image.

Downloaded by [Mizoram University] at 14:52 28 December 2015

and similarity between particle forms indicating the existence of morphological phases and homogeneous matrix. The observed particle diameters were within nanoscale range, as compared with the scale bar. Also, the Pt(IV) complex particles are smaller than Pt(II) one. The aforementioned characteristics may be considered an introductory step in applications on such nanoparticles.

4.9. *Molecular modeling*

An attempt to gain better insight on the most suitable geometry of the ligand to propose the bonding mode was carried out. Here, we calculate some parameters and the results are in accord with the experimental data. Atomic charges and optimized geometrical structures are calculated. Molecular energetic parameters, shown in table 6, display the high probability for the presence of keto–enol tautomer forms based on their similar calculated energies (figure 1). The atomic charges on the donors of the ligand (nitrogen, oxygen, and sulfur) indicate that the most negatively charged is O9 and then S12. In enol form, both S12 and N8 have almost the same value and O9 is less (table 7). This agrees with the coordination behavior of the ligand keto–enol forms. Finally, the optimized structure of the keto form is clearly angular where the phenyl rings are almost parallel to each other, close to the X-ray structure of an analogous compound [52, 53]. Metal complexes were optimized using semi-empirical PM3 method. As shown in figures 3 and 4, the optimized structure of Co(II) is tetrahedral, of Cu(II) and Ni(II) octahedral, while of Pd(II) square–planar. In these complexes, the ligand exists in enol form and coordinates to the metal ion via oxygen and sulfur. The atomic charge data indicate that both O9 and S12 become positively charged in all complexes due to coordination. On the other hand, N8, which has negative charge in the free ligand (enol form), becomes positively charged in all complexes, while N11 became slightly negative. All these foundations indicate the presence of charge-transfer L–M form which is clearly confirmed by the positive charge on the metal ion in all complexes (table 7).

Table 6. The molecular energy parameters of the ligand and its metal complexes.

Compound	Total energy	Binding energy	Electronic energy	Heat of formation	Dipole moment
$Ligand_{(Keto)}$	−67969.53	−3300.91	−455665.27	45.62	5.42
$Ligand_{(Enol)}$	−67971.32	−3302.70	−421819.72	43.83	4.24
Co	−153346.43	−6679.99	−1361832.51	11.27	7.541
Cu	−203302.21	−7997.77	−2150205.26	10.40	7.151
Ni	−174106.55	−7023.73	−1699529.00	−4.54	9.954
Pd	−159784.63	−6846.43	−1419721.75	−115.47	4.321

Table 7. Mulliken atomic charges of selected atoms of ligand and its complexes.

	N8	O9	N11	S12	Cl19	M
Keto-form	−0.0367	−0.3243	0.2596	−0.2766	0.0897	–
Enol-form	−0.3501	−0.2895	0.3233	−0.3586	0.0787	–
Co	0.2474	0.0684	−0.0599	0.0924	0.0499	−0.2699
Cu	0.2575	0.0138	0.3695	0.2186	0.0479	−0.4584
Ni	0.2078	0.1267	−0.0998	0.0847	0.0404	−0.7030
Pd	0.3110	0.2219	−0.0936	0.0138	0.0642	−0.0891

Downloaded by [Mizoram University] at 14:52 28 December 2015

5. Conclusion

Metal complexes were prepared using 1-benzoyl-3-(4-chlorophenyl) thiourea. Spectroscopic techniques were used to characterize the complexes after analysis of the free ligand. The ligand is coordinated as a neutral bidentate in Pt(IV), Pd(II), and Pt(II) complexes and mono-negative bidentate in Co(II) and Ni(II) complexes. The TEM images for platinum complexes show nanoparticles and homogeneous metal ion distribution on the complex surface. In the ESR spectrum of Cu(II) complex, the spin Hamiltonian parameters support octahedral geometry. Molecular modeling was performed implementing semi-empirical PM3 force field in Hyper-Chem 7.5 to display the most stable structural formulas. Theoretical parameters calculated support the experimental data.

Downloaded by [Mizoram University] at 14:52 28 December 2015

Supplemental data

Supplemental data for this article can be accessed here [http://dx.doi.org/10.1080/00958972.2015.1004325].

References

[1] M.A. Ali, S.E. Livingiston. *Coord. Chem. Rev.*, **13**, 273 (1974).
[2] A. Saxena, R.D. Pike. *J. Chem. Crystallogr.*, **37**, 755 (2007).
[3] X.X. Zhou, Y.M. Liang, F.J. Nan, Y.X. Ma. *Polyhedron*, **11**, 447 (1992).
[4] Y. Omote. *Bull. Chem. Soc. Jpn.*, **46**, 2896 (1973).
[5] B. Garg. *Inorg. Chim. Acta*, **170**, 177 (1990).
[6] U. El-Ayaan. *J. Mol. Struct.*, **998**, 11 (2011).
[7] M.G. Fisher, P.A. Gale, M.E. Light, R. Quesada. *CrystEngComm*, **10**, 1180 (2008).
[8] S. Nadeem, M.K. Rauf, M. Bolte, S. Ahmad, S.A. Tirmizi, M. Asma, A. Hameed. *Transition Met. Chem.*, **35**, 555 (2010).
[9] P.A. Gale, M.E. Light, R. Quesada. *CrystEngComm*, **8**, 178 (2006).
[10] P.A. Gale, M.E. Light, R. Quesada. *Chem. Commun.*, **7**, 5864 (2005).
[11] P.A. Gale, M.E. Light, R. Quesada. *Polyhedron*, **25**, 901 (2006).
[12] L.B. Kumbhare, U.S. Beena, G. Singh, A. Wadawale, G. Kedarnath, S.S. Zade, K.I. Priyadarsini, V.K. Jain. *Inorg. Chim. Acta*, **374**, 69 (2011).
[13] S.T. Cheng, E. Doxiadi, R. Vilar, A.J.P. White, D.J. Williams. *J. Chem. Soc., Dalton Trans.*, 2239 (2001).
[14] P. Diaz, D.M.P. Mingos, R. Vilar, A.J.P. White, D.J. Williams. *Inorg. Chem.*, **43**, 7597 (2004).
[15] E. Wong, C.M. Giandomenico. *Chem. Rev.*, **99**, 2451 (1999).
[16] Y. Jung, S.J. Lippard. *Chem. Rev.*, **107**, 1387 (2007).
[17] J. Kozelka, F. Legendre, F. Reeder, J.C. Chottard. *Coord. Chem. Rev.*, **190–192**, 61 (1999).
[18] J. Reedijk. *Chem. Rev.*, **99**, 2499 (1999).
[19] R.T. Dorr. In *A Review of the Modulation of Cisplatin Toxicities in by Chemoprotectants. Platinum and other Metals Coordination Compounds in Cancer Chemotherapy 2*, H.M. Pinedo, J.H. Schornagel (Eds.), Plenum Press, New York, NY (1996).
[20] M. Bloemink, J. Reedijk. In *Metal Ions in Biological Systems; Cisplatin and Derived Anticancer Drugs. Mechanism and Current Status of DNA Binding*, A. Sigel, H. Sigel (Eds.), Marcel Dekker, New York, NY (1996).
[21] K.A. Mitchell, C.M. Jensen. *Inorg. Chim. Acta*, **265**, 103 (1997).
[22] N.L. Allinger. *J. Am. Chem. Soc.*, **99**, 8127 (1977).
[23] *Hyper-Chem Professional 7.5*, Hypercube, Inc., Gainesville, FL, 2002. Available online at: http://www.hyper.com.
[24] A.I. Vogel. *Text Book of Quantitative Inorganic Analysis*, Longman, London (1986).
[25] W.J. Geary. *Coord. Chem. Rev.*, **7**, 81 (1971).
[26] M.S. Refat. *Spectrochim. Acta, Part A*, **68**, 1393 (2007).
[27] N.M. El Metwally, R. Arafa, U. El-Ayaan. *J. Therm. Anal. Calorim.*, **8**, 3065 (2013).
[28] U. El-Ayaan, M.M. Youssef, S. Al-Shihry. *J. Mol. Struct.*, **936**, 213 (2009).
[29] K.S. Siddiqi, R.I. Kureshy, N.H. Khan, S. Tabassum, S.A.A. Zaidi. *Inorg. Chim. Acta*, **151**, 95 (1988).

[30] S. Tabassum, K.S. Siddiqi, N.H. Khan, R.I. Kureshy, S.A.A. Zaid. *Ind. J. Chem.*, **26A**, 523 (1987).
[31] S.J. Swamy, K. Bhaskar. *Ind. J. Chem.*, **38A**, 961 (1999).
[32] A.A. El-Asmy, A.Z. El-Sonbati, A.A. Ba-Issa. *Transition Met. Chem.*, **15**, 222 (1990).
[33] R. Srinivasan, I. Sougandi, R. Venkatesan, P. Rao. *J. Chem. Sci.*, **115**, 91 (2003).
[34] S. Chandrasekhar, A. McAuley. *Inorg. Chem.*, **31**, 2234 (1992).
[35] M.S. Masoud, S.A. Abou El-Enein, M.E. Ayad, A.S. Goher. *Spectrochim. Acta, Part A*, **60**, 77 (2004).
[36] A.B.P. Lever. *Inorganic Electronic Spectroscopy*, 2nd Edn, Elsevier, Amsterdam (1984).
[37] A.A. El-Asmy, M.E. Khalifa, M.M. Hassanian. *Synth. React. Inorg. Met.-Org. Chem.*, **31**, 1787 (2001).
[38] E. Franco, E. López-Torres, M.A. Mendiola, M.T. Sevilla. *Polyhedron*, **19**, 441 (2000).
[39] A.B.P. Lever. *Inorganic Electronic Spectroscopy*, Elsevier, Amsterdam (1986).
[40] J.P. Jasinski, J.R. Bianchani, J. Cueva, F.A. El-Saied, A.A. El-Asmy, D.X. West. *Z. Anorg. Allg. Chem.*, **629**, 202 (2003).
[41] G. Speier, J. Csihony, A.M. Whalen, C.G. Pierpont. *Inorg. Chem.*, **35**, 3519 (1996).
[42] B.J. Hathaway, D.E. Billing. *Coord. Chem. Rev.*, **5**, 143 (1970).
[43] J.A. Welleman, F.B. Hulsbergen. *J. Inorg. Nucl. Chem.*, **40**, 143 (1978).
[44] H. Yokoi, A.W. Addison. *Inorg. Chem.*, **16**, 1341 (1977).
[45] R.K. Ray, G.R. Kauffman. *Inorg. Chim. Acta*, **173**, 207 (1990).
[46] R.C. Chikate, S.B. Padhye. *Polyhedron*, **24**, 1689 (2005).
[47] R.C. Maurya, S. Rajput. *J. Mol. Struct.*, **687**, 35 (2004).
[48] A.A. Fahem. *Spectrochim. Acta, Part A*, **88**, 10 (2012).
[49] A. Shahrjerdi, S.S. Hosseiny Davarani, E. Najafi, M.M. Amini. *Ultrason. Sonochem.*, **22**, 382 (2015).
[50] B.D. Cullity, *Elements of X-ray Diffraction*, 3rd Edn, Addison-Wesley Inc., Boston, MA (1993).
[51] B.D. Cullity, *Elements of X-ray Diffraction*, 2nd Edn, Addison-Wesley Mass, Boston, MA (1978).
[52] M.H. Abdel-Rhman, M.M. Hassanian, A.A. El-Asmy. *J. Mol. Struct.*, **1019**, 110 (2012).
[53] H. Beraldo, W.F. Nacif, D.X. West. *Spectrochim. Acta, Part A*, **57**, 1847 (2001).

Downloaded by [Mizoram University] at 14:52 28 December 2015